



© 2015 IEEE

IEEE Wireless Communications Letters Vol. 4, Issue 3, June 2015

DOI: [10.1109/LWC.2015.2412941](https://doi.org/10.1109/LWC.2015.2412941)

## **Novel dynamic and static methods for out-of-band power suppression in SC-OFDM**

F. Hasegawa  
A. Okazaki  
A. Okamura  
D. Castelain  
C. Ciochina-Duschene  
L. Brunel  
D. Mottier

Personal use of this material is permitted. Permission from IEEE must be obtained for all other uses, in any current or future media, including reprinting/republishing this material for advertising or promotional purposes, creating new collective works, for resale or redistribution to servers or lists, or reuse of any copyrighted component of this work in other works."

# Novel Dynamic and Static Methods for Out-of-Band Power Suppression in SC-OFDM

Fumihiko Hasegawa, Akihiro Okazaki, Atsushi Okamura,  
Damien Castelain, Cristina Ciochina-Duchesne, Loïc Brunel, and David Mottier

**Abstract**—Novel dynamic and static out-of-band (OoB) suppression methods for single carrier (SC)-orthogonal frequency division multiplexing (OFDM) are proposed in this letter. In the dynamic approach, symbols at designated positions from the previous block are inserted at predetermined positions in the current block to maintain continuity between blocks. In the static method, a fixed sequence of symbols is inserted in an SC-OFDM block for OoB power suppression. In both approaches, OoB power can be suppressed significantly by controlling design parameters.

**Index Terms**—SC-OFDM, out-of-band emissions, phase continuity

## I. INTRODUCTION

Single carrier (SC)-orthogonal frequency division multiplexing (OFDM), a full carrier version of SC-FDMA (Frequency Division Multiple Access) [1], is an attractive block transmission method due to its low envelope variations and robust performance against multipath fading channels. However, inheriting the phase discontinuity problem from OFDM, out-of-band (OoB) emissions becomes a problem in SC-OFDM. Windowing techniques [2] reduce useful portions of cyclic prefix (CP). A variety of techniques [3] [4] have been proposed to lower the OoB emission for OFDM but they cannot be directly applied to SC-OFDM. The authors in [5] proposed ECP-OFDM (extended cyclic prefix OFDM) which extends OFDM blocks into neighboring blocks for smoother phase transition by adding perturbation vectors to OFDM signals. In this letter, novel methods are proposed to create overlapping SC-OFDM blocks simply by using the past symbols or static sequences to improve continuity of the waveform and lower the OoB emission.

## II. PROPOSED OOB SUPPRESSION METHODS

### A. Signal model and measure of continuity

The signal model and measure of continuity are described here. The number of data symbols, length of CP and number of carriers for an SC-OFDM block are denoted as  $N_D$ ,  $N_{CP}$  and  $N$ , respectively. First, discrete Fourier transform (DFT) precoding is applied to  $N_D$  data symbols  $\mathbf{d}_k = [d_{k,0}, \dots, d_{k,N_D-1}]^T$  for the  $k^{\text{th}}$  block obtaining  $s_{k,l} = \sum_{m=0}^{N_D-1} e^{-j2\pi ml/N_D} d_{k,m}$  where  $-N_D/2 \leq l \leq N_D/2 - 1$ .

F. Hasegawa, A. Okazaki and A. Okamura are with Mitsubishi Electric Corporation, Information Technology R & D Center, Kamakura, Kanagawa 247-8501, Japan. (e-mail: Hasegawa.Fumihiko@bk.MitsubishiElectric.co.jp).

D. Castelain, C. Ciochina-Duchesne, L. Brunel and D. Mottier are with Mitsubishi Electric R&D Centre Europe, CS 10806, 35708 Rennes Cedex 7, France.

It is assumed that  $E[|d_{k,i}|^2] = 1$  and  $E[d_{k,m}d_{l,n}^*] = 0$  if  $k \neq l$  or  $m \neq n$ . The precoded symbols are mapped onto  $N_D$  carriers with  $(N - N_D)/2$  zeros on each side as a guard band. Subsequently,  $N$  carriers are converted to time-domain signals by the inverse discrete Fourier transform (IDFT). Denoting  $x_k(t)$ ,  $T_{CP}$  and  $T_S$  as OFDM signal for the  $k^{\text{th}}$  block, duration of CP and block interval without CP, respectively, it has been shown in [4] that OoB power suppression for OFDM can be achieved by setting derivatives of the signal continuous at block transitions so that  $x_k^{(p)}(-T_{CP}) = x_{k-1}^{(p)}(T_S)$ , where  $x_k^{(p)}(t)$  denotes the  $p^{\text{th}}$  derivative of  $x_k(t)$  and  $x_k(t)$  is assumed to be nonzero for  $-T_{CP} \leq t \leq T_S$ . Using the analog representation of the OFDM signal used in [4], an analog representation of an SC-OFDM waveform for the  $k^{\text{th}}$  block is given by  $x_k(t) = \sum_{l=-N_D/2}^{N_D/2-1} s_{k,l} e^{j2\pi l \frac{t}{T_S}}$ . Substituting the definition of  $s_{k,l}$  in  $x_k(t)$ , it can be shown that  $x_k(t) = \sum_{m=0}^{N_D-1} d_{k,m} \sum_{l=-N_D/2}^{N_D/2-1} e^{-j2\pi l (\frac{m}{N_D} - \frac{t}{T_S})}$ . Let us assume that  $T_{CP}$ ,  $T_S$  and  $N_D$  are chosen such that the following condition is satisfied,

$$\frac{T_{CP}}{T_S} = \frac{T \cdot N_{CP}}{T \cdot N} = \frac{\chi}{N_D}, \quad (1)$$

where  $T$  is the sampling time  $T = T_S/N$  and  $\chi$  is an integer. Then, it is obvious that  $x_k(-T_{CP}) = N_D \cdot d_{k,N_D-\chi}$ . It can be shown that  $x_k^{(p)}(t) = \sum_{m=0}^{N_D-1} d_{k,m} \alpha_m^{(p)}(t)$  where  $\alpha_m^{(p)}(t) = \left(\frac{j2\pi}{T_S}\right)^p \sum_{l=-N_D/2}^{N_D/2-1} l^p e^{-j2\pi l (\frac{m}{N_D} - \frac{t}{T_S})}$ . If the condition in (1) is satisfied,  $\alpha_m^{(p)}(-T_{CP})$  can be expressed as  $\alpha_m^{(p)}(-T_{CP}) = \left(\frac{j2\pi}{T_S}\right)^p \sum_{l=-N_D/2}^{N_D/2-1} l^p e^{-\frac{j2\pi l}{N_D}(m+\chi)}$ . In addition,  $\alpha_m^{(p)}(T_S)$  can be written as  $\alpha_m^{(p)}(T_S) = \left(\frac{j2\pi}{T_S}\right)^p \sum_{l=-N_D/2}^{N_D/2-1} l^p e^{-\frac{j2\pi l m}{N_D}}$ . Then, the following equality can be derived,  $\alpha_m^{(p)}(T_S) = \alpha_{\text{mod}(m-\chi, N_D)}^{(p)}(-T_{CP}) = \alpha_m^{(p)}$ , where  $\text{mod}(x, y)$  denotes “ $x$  modulo  $y$ ” and  $\alpha_m^{(p)}$  is introduced for notational convenience. Let us also define an error term which is used as a measure of continuity in this letter,  $\varepsilon^{(p)} = x_k^{(p)}(-T_{CP}) - x_{k-1}^{(p)}(T_S)$ . By using the definition of  $x_k^{(p)}(t)$  and  $\alpha_m^{(p)}$ , the error term  $\varepsilon^{(p)}$  can be written as

$$\varepsilon^{(p)} = \sum_{m=0}^{N_D-1} \alpha_m^{(p)} \underbrace{(d_{k, \text{mod}(m-\chi, N_D)} - d_{k-1, m})}_{\beta_m}. \quad (2)$$

### B. Proposed dynamic method

1) *Symbol design*: The goal here is to extend an SC-OFDM block into adjoining blocks to create overlapping regions so

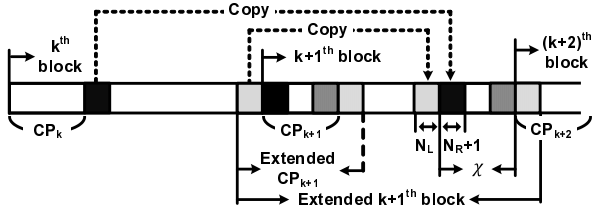


Fig. 1. SC-OFDM block format in the proposed dynamic method

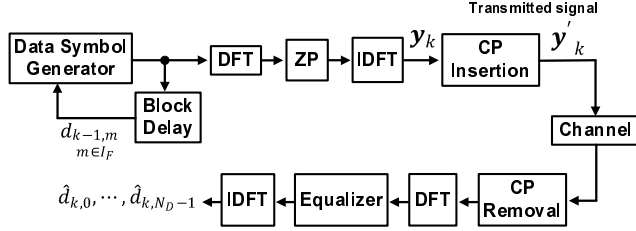


Fig. 2. Proposed transmitter and receiver with the dynamic method

that interblock continuity is improved. Simultaneously, similar to the method in [5], cyclicity needs to be preserved within the extended SC-OFDM block to create an extended CP. Thus, the following symbol placement is proposed:

$$\begin{aligned} d_{k,N_D-\chi+m} &= d_{k-1,m}, & 0 \leq m \leq N_R \\ d_{k,N_D-\chi-n} &= d_{k-1,N_D-n}, & 1 \leq n \leq N_L \end{aligned} \quad (3)$$

where  $N_R$  and  $N_L$  determine size of the overlapping region. If we define  $N_F = N_R + N_L + 1$  and  $N_F \leq \chi$ ,  $N_D - N_F$  symbols are reserved for new data symbols in (3). It is obvious from (3) that  $\beta_m = 0$  is achieved in (2) for  $m \in I_F$  where  $I_F = \{0, 1, \dots, N_R, N_D - N_L, \dots, N_D - 1\}$ . An example of the proposed block structure is illustrated in Fig. 1, where  $N_D = N$  is assumed for simplicity. It is clear from Fig. 1 that neighboring blocks are overlapped since the  $(k+1)^{th}$  block can be extended into the  $k^{th}$  and  $(k+2)^{th}$  block by  $N_L$  and  $N_R + 1$  symbols, respectively. Furthermore, cyclicity appears within the extended block, thanks to the extended CP.

When  $N_R = N_L = 0$ , the proposed method becomes  $d_{k,N_D-\chi} = d_{k-1,0}$ . Thanks to periodic extension in the IDFT output [6] [7] and condition in (1),  $x_{k-1}(T_S)$  approaches  $d_{k-1,0}$  which is also the first sample of the CP of the next block  $x_k(-T_{CP}) = N_D \cdot d_{k-1,0}$ . It is also clear from the definition of  $\alpha_m^{(p)}$  and (2) that setting  $d_{k,N_D-\chi} = d_{k-1,0}$  yields  $\varepsilon^{(0)} = 0$  since  $\alpha_m^{(0)} = 0$  for  $m \neq 0$  and  $\beta_0 = 0$ : the 0<sup>th</sup> order continuity is achieved.

The transmitter and receiver structure of the proposed method are shown in Fig. 2. As indicated in the figure, the output of the IDFT corresponding to the  $k^{th}$  block, which contains  $N$  symbols oversampled  $L$  times by zero padding (ZP) in the frequency domain, is written as  $\mathbf{y}_k = [y_{k,0}, \dots, y_{k,NL-1}]^T$ . The last  $LN_{CP}$  samples of  $\mathbf{y}_k$ , denoted as  $\mathbf{y}_{CP,k} = [y_{k,L(N-N_{CP})}, \dots, y_{k,NL-1}]^T$ , are used as CP. The transmitted signal can be written as  $\mathbf{y}'_k = [\mathbf{y}_{CP,k}^T, \mathbf{y}_k^T]^T$ . The transmitter requires a delay component which holds the designated symbols for one SC-OFDM block duration. As

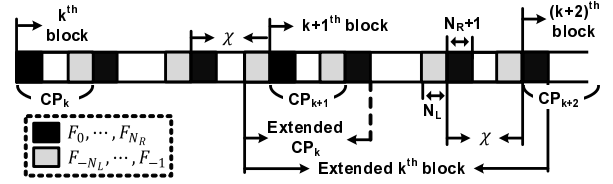


Fig. 3. SC-OFDM block format for the proposed static method

shown in Fig. 2, conventional SC-FDMA receivers [1] can be used to demodulate the proposed waveform. For example, during demodulation of the  $k^{th}$  SC-OFDM block, the demodulator may ignore  $\hat{d}_{k,N_D-\chi+m}$  for  $-N_L \leq m \leq N_R$  since these symbols are already demodulated in the previous block.

2) *Comparison with ECP-OFDM [5]*: For clarity, the transmission method proposed in [5] is described here. Let us define an  $NL \times N_D$  IDFT matrix  $\mathbf{W}$  where the  $(m, n)^{th}$  element of  $\mathbf{W}$  is given by  $[\mathbf{W}]_{m,n} = e^{j2\pi m i_n / NL}$  and  $i_n \in \{0, \dots, N_D/2 - 1, NL - N_D/2, \dots, NL - 1\}$ . Then an OFDM waveform for the  $k^{th}$  block can be expressed as  $\mathbf{r}_k = [r_{k,0}, \dots, r_{k,NL-1}]^T = \mathbf{W} \mathbf{d}_k$ . The perturbation vector  $\mathbf{w}_k = [w_{k,0}, \dots, w_{k,NL-1}]^T$  is added to the OFDM waveform to obtain  $\tilde{\mathbf{r}}_k = [\tilde{r}_{k,0}, \dots, \tilde{r}_{k,NL-1}]^T = \mathbf{r}_k + \mathbf{w}_k$ . Let us also represent rows between  $(N - N_{CP})^{th}$  and  $(N - N_{CP} + N_S - 1)^{th}$  row of  $\mathbf{W}$  as  $\tilde{\mathbf{W}}$  and define  $e_{k,m} = \tilde{r}_{k-1,m} - r_{k,m+(N-N_{CP})L}$  for  $m = 0, \dots, N_S - 1$  where  $N_S$  is a design parameter that determines the size of the overlapping region. The perturbation vector is computed to minimize the average power of  $\mathbf{f}_k = [f_{k,0}, \dots, f_{k,N_D-1}]^T$  where  $\mathbf{e}_k = [e_{k,0}, \dots, e_{k,N_S-1}]^T = \tilde{\mathbf{W}} \mathbf{f}_k$ . Then, assuming all data subcarriers are used to compute  $\mathbf{w}_k$ , the OFDM waveform with the perturbation vector can be expressed as  $\tilde{\mathbf{r}}_k = \mathbf{r}_k + \mathbf{W} \tilde{\mathbf{W}}^H (\tilde{\mathbf{W}} \tilde{\mathbf{W}}^H)^{-1} \mathbf{e}_k$ , where  $\tilde{\mathbf{W}}^H$  is the Hermitian transpose of  $\tilde{\mathbf{W}}$ . Since the optimum perturbation vector must be computed for every OFDM block, the receiver for ECP-OFDM needs to implement an interference cancellation algorithm to remove the perturbation vectors from the received signal to avoid BER performance degradation [5]. On the contrary, due to simple symbol assignments in the proposed method (3), OoB suppression can be achieved without any BER performance loss.

### C. Proposed static method

Defining a static sequence as  $[F_{-N_L}, \dots, F_0, \dots, F_{N_R}]$ , the proposed static method can be expressed as

$$\begin{aligned} d_{k,N_D-\chi+m} &= F_m, & d_{k-1,m} &= F_m, & 0 \leq m \leq N_R \\ d_{k,N_D-n-\chi} &= F_{-n}, & d_{k-1,N_D-n} &= F_{-n}. & 1 \leq n \leq N_L \end{aligned} \quad (4)$$

The proposed static sequence placement is shown in Fig. 3. In the proposed SC-OFDM block,  $2N_F$  data symbols are replaced with the static sequence and  $N_D - 2N_F$  symbols are reserved for new data symbols. Similar to the dynamic method, it is clear from Fig. 3 that the proposed block can be extended into adjacent blocks. It is also clear from (4) that  $\beta_m = 0$  can be obtained in (2) for  $m \in I_F$ . An advantage of the proposed

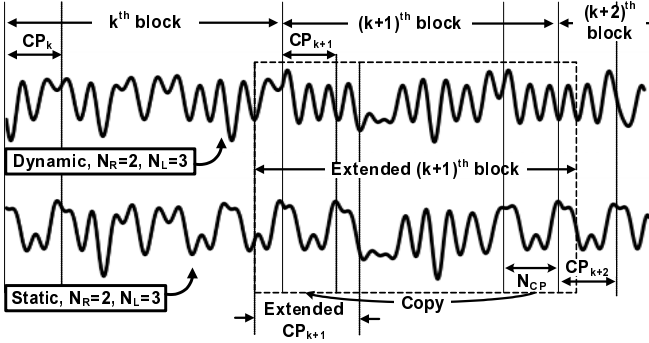


Fig. 4. Waveforms generated by the dynamic and static method with  $N_D = 24, N = 32, N_{CP} = 8$  for  $N_R = N_L = 2$

method over a dynamic method is that the conventional SC-OFDM transmitter can be configured to replace data symbols with the static sequence. However,  $2N_F$  symbols are reserved for the static sequence whereas only  $N_F$  symbols are used for the past symbols in the dynamic method. It should be noted that when  $N_R = N_L = 0$ , the proposed static sequence becomes  $d_{k, N_D - \chi} = d_{k-1, 0} = F_0$ , resembling two “anchor symbols” placed in an SC-OFDM block to maintain phase continuity between blocks [7].

#### D. Performance analysis

1) *Comparison of waveforms:* An example is shown in Fig. 4 to illustrate the proposed waveforms generated by the proposed dynamic and static method. The real part of  $\mathbf{y}'_k$  for quadrature phase shift keying (QPSK) is shown in the figure. In this letter, the Zadoff-Chu sequence [8] is used for the static sequence such that  $[F_0, \dots, F_{N_R}, F_{-N_L}, \dots, F_{-1}] = [1, \dots, e^{-\frac{j\pi k^2}{N_F}}, \dots, e^{-\frac{j\pi(N_F-1)^2}{N_F}}]$ . From the figure, it is clear that phase transition can be improved by the proposed methods, thanks to the extended SC-OFDM block. Furthermore, it is noticeable from the figure that the overlapping regions in the static method are composed of the static sequences and remain fixed whereas overlapping regions in the dynamic method change randomly. We note from the figure that due to the inter-symbol interference [9], extended CP becomes an approximate CP when  $N_D < N$ .

2) *MSE performance analysis for the dynamic method:* Let us evaluate the mean square error (MSE) performance of the proposed dynamic method using  $\varepsilon^{(p)}$  in (2). It can be shown that MSE for SC-OFDM is given by  $\bar{\varepsilon}^{(p)} = E[|\varepsilon^{(p)}|^2] = 2 \sum_{m=0}^{N_D-1} |\alpha_m^{(p)}|^2$ , where  $E[|\beta_m|^2] = 2$ . Note from (2) that MSE can be reduced by setting  $\beta_m = 0$  for selected values of  $m$ . Thus, using (2) and (3), MSE for the proposed method can be written as  $\bar{\varepsilon}^{(p)} = 2 \sum_{m \notin I_F} |\alpha_m^{(p)}|^2$ . Hence, reduction of MSE by  $2 \sum_{m \in I_F} |\alpha_m^{(p)}|^2$  can be achieved with the proposed dynamic method. Theoretical MSE  $\bar{\varepsilon}^{(p)}$  of the dynamic method, evaluated with the parameters from DVB-NGH [10], is shown in Table I. For each value of  $p$ , all MSE performances of the proposed method are normalized by the

TABLE I  
THEORETICAL MSE (IN DB) OF THE DYNAMIC METHOD WHEN  
 $N_D = 432, N = 512, N_{CP} = 32$  [10] AND  $\chi = 27$

$p$	1	2	3	4
$N_R = N_L = 0$	0.0	-3.5	0.0	-1.9
$N_R = 1, N_L = 2$	-5.0	-16.8	-1.8	-9.2
$N_R = 11, N_L = 12$	-13.0	-40.9	-9.3	-32.4

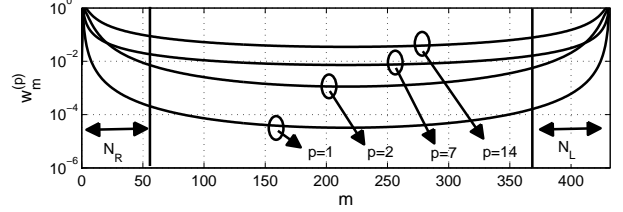


Fig. 5.  $\omega_m^{(p)}$  for  $p = \{1, 2, 7, 14\}$  when  $N_D = 432$

MSE performance of SC-OFDM with no OoB suppression technique. Theoretical MSE for  $p = 0$  is not shown in the table since the proposed methods achieve the 0<sup>th</sup> order continuity. It is clear from Table I that the MSE performances for all values of  $p$  can be improved by increasing  $N_R$  and  $N_L$ .

Improvement in the MSE performance by increasing  $N_R$  and  $N_L$  can be explained by investigating  $\alpha_m^{(p)}$ . It is clear from the definition of  $\alpha_m^{(p)}$  that  $\alpha_m^{(p)}$  is the  $m^{\text{th}}$  coefficient of the DFT of  $l^p$ . In Fig. 5, normalized  $|\alpha_m^{(p)}|^2$ ,  $\omega_m^{(p)} = \frac{|\alpha_m^{(p)}|^2}{\max |\alpha_n^{(p)}|^2}$ , is shown for various values of  $p$  when  $N_D = 432$ . From the figure, it is clear that  $\omega_m^{(p)}$  decreases as  $m$  approaches  $N_D/2$  and signal energy of  $l^p$  in the frequency domain is concentrated mainly near  $m = 0$ . As  $p$  increases, the energy distribution of  $l^p$  flattens due to the presence of higher frequency components in  $l^p$ . Thus, more reduction in MSE can be obtained by increasing  $N_R$  and  $N_L$  in (3) since, as indicated in Fig. 5,  $N_R$  and  $N_L$  in (3) can be interpreted as bandwidth of a lowpass filter capturing energy in  $\alpha_m^{(p)}$ .

3) *Performance analysis for the static method:* MSE performance analysis of the static method is not straightforward due to the presence of the proposed static sequence. Thus, let us present the following upper bound of  $|\varepsilon^{(p)}|^2$  using the Cauchy-Schwarz inequality [11],  $|\varepsilon^{(p)}|^2 \leq \varepsilon_{UB}$  where  $\varepsilon_{UB} = \left( \sum_{m=0}^{N_D-1} |\alpha_m^{(p)}|^2 \right) \left( \sum_{m=0}^{N_D-1} |\beta_m|^2 \right)$ . Note from (2) that the upper bound  $\varepsilon_{UB}$  can be reduced by setting  $\beta_m = 0$  for selected values of  $m$ . Thus, with the proposed static method (4), the following upper bound can be obtained  $|\varepsilon^{(p)}|^2 \leq \left( \sum_{m \notin I_F} |\alpha_m^{(p)}|^2 \right) \left( \sum_{m \notin I_F} |\beta_m^{(p)}|^2 \right) < \varepsilon_{UB}$ . Clearly, reduction in the upper bound by  $\sum_{m \in I_F} |\alpha_m^{(p)}|^2$  is achieved with the proposed method (4).

### III. SIMULATION RESULTS

The power spectra of the proposed signals obtained through simulations (Sim.) and experiments (Exp.) are shown in Fig. 6. The parameters considered in DVB-NGH with QPSK modulation is used. In the simulation, the spectra are estimated

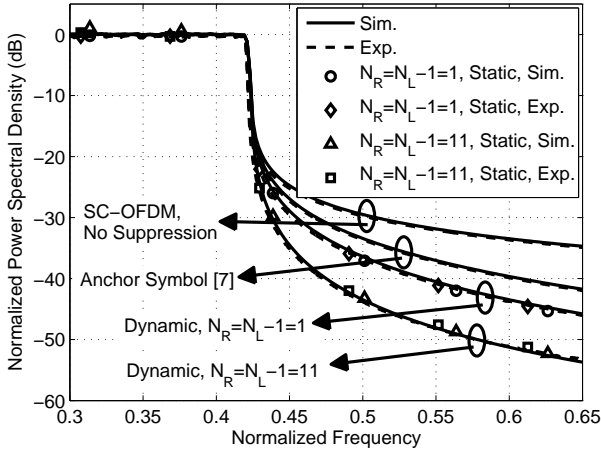


Fig. 6. OoB suppression performance of the proposed methods,  $N_D = 432$ ,  $N = 512$ ,  $N_{CP} = 32$  [10] and  $\chi = 27$

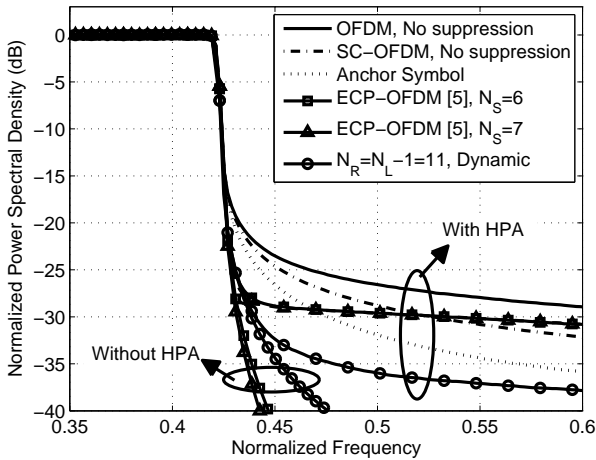


Fig. 7. OoB suppression performance of the proposed methods in the presence of HPA,  $N_D = 432$ ,  $N = 512$ ,  $N_{CP} = 32$  [10] and  $\chi = 27$

with the Welch's averaged periodogram method with  $L = 4$ , an  $NL$ -sample Hann window [6] and  $\frac{NL}{8}$ -sample overlap. In the experiment, signal bandwidth of 5MHz is assumed. Anritsu MG3700A and Anritsu MS2690A are used to generate waveforms and collect data, respectively. While the spectral loss for the anchor symbol method [7] is  $2/432 \approx 0.463\%$ , the spectral loss for the dynamic and static methods are  $24/432 \approx 5.56\%$  and  $48/432 \approx 11.11\%$ , respectively, when  $N_R = N_L - 1 = 11$ . It is obvious from Fig. 6 that OoB spectral suppression can be improved by increasing  $N_R$  and  $N_L$ . Furthermore, the proposed dynamic method can achieve the same OoB reduction performance as the static method with superior spectral efficiency. Finally, as can be seen from Fig. 6, simulation and experimental results are in agreement.

In Fig. 7, a comparison between power spectra of ECP-OFDM [5] and proposed method is shown. In the simulation, the Rapp model  $\left| \frac{V_{out}}{V_{in}} \right| = \left( 1 + \left| \frac{V_{in}}{V_{sat}} \right|^{2p} \right)^{-1/2p}$  [12] with

$V_{sat} = 1$  is used as the high power amplifier (HPA). Input and output amplitudes are represented by  $V_{in}$  and  $V_{out}$ , respectively. Following the simulation parameters used in [9], QPSK,  $p = 2$  and input backoff of 7dB are assumed. The OoB suppression performances of the proposed dynamic method and ECP-OFDM with  $N_S = \{6, 7\}$  are shown in Fig. 7. From Fig. 7, it is clear that due to adaptive data processing applied to every OFDM block at the transmitter, ECP-OFDM outperforms the proposed dynamic method when the HPA is not incorporated in the simulation. However, in the presence of the HPA, the suppression performance of ECP-OFDM degrades because of high peak to average power ratio (PAPR) of the OFDM waveform. Furthermore, increasing  $N_S$  does not improve the suppression performance of ECP-OFDM. On the contrary, the proposed dynamic scheme yields better OoB suppression performance compared to ECP-OFDM, thanks to low envelop variations of SC-OFDM.

#### IV. CONCLUSION

Two novel transmission methods are proposed to reduce OoB emission for SC-OFDM. While the static approach relies on insertion of a fixed sequence of symbols, the dynamic approach uses data symbols from the previous SC-OFDM block to maintain continuity between blocks. Simulation results demonstrate that the proposed methods can reduce OoB emission significantly compared to the existing methods.

#### V. ACKNOWLEDGMENT

The authors would like to thank Dr. S. Fushimi and Mr. N. Yamada of Mitsubishi Electric Corporation for their encouragement and support throughout this work.

#### REFERENCES

- [1] H. Myung, J. Lim, and D. Goodman, "Single carrier FDMA for uplink wireless transmission," *IEEE Veh. Technol. Mag.*, vol. 1, no. 3, pp. 30–38, Sept. 2006.
- [2] M. Faulkner, "The effect of filtering on the performance of OFDM systems," *IEEE Trans. Veh. Technol.*, vol. 49, no. 5, pp. 1877–1884, Sept. 2000.
- [3] C.-D. Chung, "Spectrally precoded OFDM," *IEEE Trans. on Commun.*, vol. 54, no. 12, pp. 2173–2185, Dec. 2006.
- [4] J. van de Beek and F. Berggren, "N-continuous OFDM," *IEEE Commun. Lett.*, vol. 13, no. 1, pp. 1–3, Jan. 2009.
- [5] Y. Jiang and Y. Wang, "A new out-of-band power suppression scheme by extending effective cyclic-prefix of OFDM," in *Proc. VTC 2010*, May 2010, pp. 1–5.
- [6] B. Porat, *A Course in Digital Signal Processing*. New York, NY, USA: John Wiley & Sons, 1997.
- [7] F. Hasegawa, M. Higashinaka, A. Okazaki, F. Ishizu, D. Castelain, L. Brunel, and D. Mottier, "Phase-anchored SC-OFDM," *IEEE Wireless Commun. Letters*, vol. 3, no. 1, pp. 22–25, Feb. 2014.
- [8] D. Chu, "Polyphase codes with good periodic correlation properties," *IEEE Trans. Inf. Theory*, vol. 18, no. 4, pp. 531–532, Jul. 1972.
- [9] N. Benvenuto, R. Dinis, D. Falconer, and S. Tomasin, "Single carrier modulation with nonlinear frequency domain equalization: An idea whose time has come - again," *Proc. IEEE*, vol. 98, no. 1, pp. 69–96, Jan 2010.
- [10] "Digital video broadcasting (DVB); Next generation broadcasting system to handheld, physical layer specification (DVB-NGH)," *DVB Document A160*, Nov. 2012.
- [11] T. K. Moon and W. C. Stirling, *Mathematical Methods and Algorithms for Signal Processing*. Upper Saddle River, NJ, USA: Prentice Hall, 2000.
- [12] C. Rapp, "Effects of the HPA-nonlinearity on a 4-DPSK/OFDM signal for a digital sound broadcasting system," in *Proc. European Conf. on Satellite Commun.*, Oct. 1991, pp. 179–184.